Cancer Letters 447 (2019) 164–173

Contents lists available at ScienceDirect

Cancer Letters

journal homepage: www.elsevier.com/locate/canlet

Original Articles

# High-affinity human programmed death-1 ligand-1 variant promotes redirected T cells to kill tumor cells

Zhaoduan Liang[a], Yanyan Li[a,b], Ye Tian[a], Huanling Zhang[a,b], Wenxuan Cai[a], Anan Chen[a], Lin Chen[a], Yifeng Bao[a], Bo Xiang[c], Heping Kan[c,**], Yi Li[a,*]

[a] State Key Laboratory of Respiratory Disease, Guangzhou Institutes of Biomedicine and Health, Chinese Academy of Sciences, 190 Kai Yuan Avenue, Science Park, Guangzhou, Guangdong province, China
[b] School of Life Sciences, University of Science and Technology of China, No. 96, Jinzhai road, Hefei, Anhui province, China
[c] Department of Hepatobiliary Surgery, Nanfang Hospital, Southern Medical University, 1838, North Guangzhou Avenue, Baiyun District, Guangzhou, Guangdong province, China

ARTICLE INFO

*Keywords:*
Protein engineering
hPD-L1
T cells
Cancer
Immunotherapy

ABSTRACT

Tumor cells can escape immune surveillance through the programmed cell death protein 1 (PD-1) axis suppressing T cells. However, we recently demonstrated that high-affinity variants of soluble human programmed death-ligand 1 (shPD-L1) could diminish the suppression. We propose that in comparison to the wild-type shPD-L1, the further affinity enhancement will confer the molecule with opposite characteristics that augment T-cell activation and immunotherapeutic drug potential. In this study, a new shPD-L1 variant, L3C7c, has been generated to demonstrate ~167 fold greater affinity than wild-type hPD-L1. The L3C7c-Fc fusion protein demonstrated completely opposite effects of conventional PD-1 axis by promoting redirected T-cell proliferation, activation and cytotoxicity *in vitro*, as being slightly better than that of anti-PD1-Ab (Pembrolizumab). Moreover, L3C7c-Fc was more effective than Pembrolizumab in enhancing redirected T cells' ability to suppress Mel624 melanoma growth *in vivo*. As a downsized L3C7c-Fc variant, L3C7v-Fc improved the anti-tumor efficacy *in vivo* when combined with dendritic cell vaccines. In conclusion, our studies demonstrate that high-affinity hPD-L1 variants could be developed as the next generation reagents for tumor immunotherapy based on the blockade of the PD-1 axis.

## 1. Introduction

The programmed cell death protein 1 (PD-1) axis that involves the interaction between PD-1 and PD-1 ligand-1 (PD-L1) is utilized by cancer cells to resist anti-tumor immunity [1]. PD-L1 is originally identified as a cell-surface glycoprotein [2]. The expression of PD-L1 has been found constitutively on a broad range of somatic cells [2] and the majority of human tumor cells [3,4]. The interaction of PD-L1 with PD-1 expressed on activated T cells causes the PD-1 axis to attenuate T-cell growth and cytokine secretion, leading to T-cell exhaustion and the maintenance of peripheral tolerance [2,5]. Cancer cell-associated PD-L1 increases the apoptosis of antigen-specific T cell clones *in vitro* [6] and creates tumor resistance to immunotherapy *in vivo* [7]. Moreover, the elevated levels of PD-L1 and PD-1 are closely correlated with the

*Abbreviations:* PD-1, programmed cell death protein 1; PD-L1, programmed death-ligand 1; NSCLC, advanced non-small cell lung cancer; HATac, high-affinity T-cell activation core molecules; DC, dendritic cell; PBMC, peripheral blood mononuclear cell; SPR, surface plasmon resonance; Fc, crystalizable fragments; HRP, horseradish-peroxidase; Ig, immunoglobulin; FACS, fluorescence-activated cell sorting; CFDA-SE, carboxyfluorescein diacetate succinimidyl ester; PMA, phorbol 12-myristate 13-acetate; Ion., ionomycin; LDH, lactate dehydrogenase; SHP-2, Src homology 2 based tyrosine phosphatases; SHP-1, Src homology 1 based tyrosine phosphatases; ITSM, immunoreceptor tyrosine-based switch motif; ZAP-70, ζ-associated protein of 70 kDa; PI3K, phosphatidylinositide 3-kinases; Lck, lymphocyte-specific protein tyrosine kinase; PLC-γ1, phospholipase C γ1

* Corresponding author. Guangzhou Institutes of Biomedicine and Health, Chinese Academy of Sciences, 190 Kai Yuan Avenue, Science Park, Guangzhou, Guangdong province, China.
** Corresponding author. Nanfang Hospital, Southern Medical University, 1838, North Guangzhou Avenue, Baiyun District, Guangzhou, Guangdong province, China.
*E-mail addresses:* liang_zhaoduan@gibh.ac.cn (Z. Liang), li_yanyan@gibh.ac.cn (Y. Li), tian_ye@gibh.ac.cn (Y. Tian), zhang_huanling@gibh.ac.cn (H. Zhang), cai_wenxuan@gibh.ac.cn (W. Cai), chen_anan@gibh.ac.cn (A. Chen), chen_lin@gibh.ac.cn (L. Chen), bao_yifeng@gibh.ac.cn (Y. Bao), 359521194@qq.com (B. Xiang), khp5513@126.com (H. Kan), li_yi@gibh.ac.cn (Y. Li).

https://doi.org/10.1016/j.canlet.2019.01.016
Received 25 October 2018; Received in revised form 17 December 2018; Accepted 14 January 2019
0304-3835/ © 2019 Elsevier B.V. All rights reserved.

progression, poor prognosis, and reduced overall survival of various human cancers [3,4].

Recently, blockading inhibitory immune checkpoints has been considered a promising immunotherapy approach, as it enhances the immune response to cancer. Various studies have shown that blockading the PD-1/PD-L1 interaction using anti-PD-1/PD-L1 antibodies or soluble PD-1 can rescue T cells from a functional exhaustion state, enhance anti-tumor immunity and inhibit tumor growth [8–10]. Currently, Pembrolizumab (anti-PD-1 antibody) has been approved by the Food and Drug Administration for clinical treatment of advanced non-small cell lung cancer (NSCLC) [11]. Although that immuno-oncology agent delivers significantly longer overall survival and higher objective response rates than docetaxel [11], monoclonal antibodies have difficulty entering the tumor sites due to their large size (~150 KDa), which leads to suboptimal anti-tumor efficacy [10]. Although significant T-cell suppression was observed during the binding of wild-type soluble hPD-L1 to membrane-bound PD-1, our previous study found that high-affinity soluble hPD-L1 produced diminished hPD-1 suppressive effects [12]. In this study, we obtained a new hPD-L1 variant, L3C7c, that exhibited greater affinity enhancement than the previously reported molecules [12]. We sought to determine whether the new high-affinity hPD-L1 variant might exhibit completely opposite effects in comparison to the low affinity wild-type molecule. Furthermore, a variant with smaller size (~75 KDa) and superior permeability might be able to improve anti-tumor responses with other immunotherapeutic strategies.

High-affinity T-cell activation core (HATac)-NYE is a new soluble bi-specific agent that combines ultra-high-affinity TCR with an anti-CD3 single chain antibody. It can redirect T cells to specifically recognize and kill target cells [13]. On the other hand, dendritic cells (DCs) are considered to be the most potent antigen-presenting cells and used as vaccines to powerfully initiate specific immune response against tumors. The efficacy of DC against tumors can be improved by blockading PD-1/PD-L1 immune checkpoints [8]. Thus, the combination of high-affinity hPD-L1 variants with either HATac-NYE molecule or DC vaccines is potential developments for cancer immunotherapy strategies. Our results revealed that high-affinity hPD-L1 variants could be used to blockade the PD-1 axis and improve tumor suppression by both HATac and vaccines *in vivo*. These results provide the foundation for optimizing clinical applications.

## 2. Materials and methods

### 2.1. Mice and cell lines

BALB/c mice (Female; 8 weeks old; 18 ± 2 g) were purchased from Vital River Laboratories. NOD-SCID-B2m$^{null}$ mice (Female; 8 weeks old; 20 ± 3 g) were purchased from the Model Animal Research Center of Nanjing University. The CT26 cells were purchased from the Chinese Academy of Sciences Shanghai Cell Resource Center. The Mel624 cells (HLA-A*0201$^+$NY-ESO-1$^+$) were kindly provided by Prof. Cassian Yee (MD Anderson Cancer Center, USA). The NCI-H1299 cells (HLA-A*0201$^+$NY-ESO-1$^+$) were generated by transfecting NCI-H1299 cells with HLA-A*0201, which were purchased from the Chinese Academy of Sciences Shanghai Cell Resource Center. The cell lines were treated with M-Plasmocin (Invivogen) for 1 week after resuscitation, cultured continuously for less than 2 months, and authenticated for characteristic markers and growth properties as described previously. Mycoplasma testing was performed monthly using PCR. The tumor cell lines were grown in Dulbecco's modified Eagle's medium (Gibco) supplemented with 10% heat-inactivated fetal bovine serum (FBS; Gibco) at 37 °C in a humidified 5% $CO_2$ incubator. Human peripheral blood samples of anonymous healthy donors were obtained from the Guangzhou Blood Center. Peripheral blood mononuclear cells (PBMCs) were isolated by Ficoll-Hypaque gradient centrifugation and maintained in RPMI-1640 medium (Gibco) supplemented with 10% FBS at 37 °C in a humidified 5% $CO_2$ incubator.

### 2.2. Fluorescence-activated cell sorting (FACS)

Cell-surface staining and intracellular staining were executed as previously described [12]. The experiments used the following reagents: Carboxyfluorescein diacetate succinimidyl ester (CFDA-SE; Molecular Probes); antibodies specific for human CD3-FITC (Clone UCHT1), PD-1-PE (Clone EH12.1), PD-L1-PE-Cy™7 (Clone MIH1), IFN-γ-PE (Clone B27), IL-2-APC (Clone MQ1-17H12), CD25-PE (Clone M-A251), CD107a-Alexa Fluor® 647 (Clone H4A3), active caspase-3-Alexa Fluor® 647 (Clone C92-605); for mouse PD-L1-PE (Clone MIH5), PD-1-PE (Clone J43). Non-reactive isotype matched antibodies served as controls. All of the antibodies were purchased from BD Biosciences. Fluorescence was evaluated by FACS analysis using BD Accuri™ C6 within 4 h after cell staining and the data were analyzed using FlowJo software (Tree Star).

### 2.3. PD-L1-Fc and L3C7c-Fc proteins binding to PD-1 on cells confirmed by competitive assays

The experiment was performed as previously described [12]. Briefly, human PBMCs and lymph node cells from BALB/c mice were stimulated with phorbol 12-myristate 13-acetate (PMA; Sigma-Aldrich) and ionomycin (Ion.; Sigma-Aldrich) for 24 h and 48 h. Human PBMCs were simultaneously added with either hPD-L1-Fc or L3C7c-Fc at serial concentrations (0.067 μM, 0.2 μM, 0.6 μM, 1.2 μM, 2.4 μM and 5.4 μM) combined with anti-human PD-1-PE (5 μL; Clone EH12.1). The murine lymph node cells were simultaneously supplemented with L3C7c-Fc (0.8 μM) combined with anti-mouse PD-1-PE (4 μg/mL; Clone J43). Fluorescence was evaluated by FACS.

### 2.4. Cell assays

Human PBMCs were co-cultured with either NCI-H1299 cells or Mel624 cells in the presence or absence of HATac-NYE (1 nM) at the E:T ratio of 5:1. For the lactate dehydrogenase (LDH) assay, as anti-PD-1 antibody at 10 μg/mL was reported to verify PD-1 axis blockade *in vitro* [7,14], serial concentrations (5 μg/mL, 10 μg/mL and 20 μg/mL) of hPD-L1-Fc, L3C7c-Fc, anti-PD1-Ab (Pembrolizumab; Supplemental Fig. 1) prepared as reported [15] or IgG4 (Merck-Millipore) were added and incubated for 24 h. The LDH release was tested using the CytoTox 96® non-radioactive cytotoxicity kit (Promega), and the percentage lysis was calculated according to the manufacturer's instructions. For the incucyte assay, 10 μg/mL of hPD-L1-Fc, L3C7c-Fc, Pembrolizumab or IgG4 was added in the presence of YOYO®-3 Iodide (1:10000 dilution; Invitrogen) for 72 h. Images were taken every 2 h, and the number of apoptotic cells per mm$^2$ was quantified using YOYO®-3 Iodide and the IncuCyte ZOOM (Essen Bioscience) as previously described [16]. All conditions were assayed in triplicate. The cells were incubated with either hPD-L1-Fc (10 μg/mL) or L3C7c-Fc (10 μg/mL) for 8 h in the active caspase 3 assay, and 24 h in the cytokines and active markers assay by FACS. To analyze proliferation and IFN-γ secretion, the PBMCs alone were stimulated using a combination of anti-CD3 Ab (Clone OKT3; Biolegend) and anti-CD28 Ab (Clone CD28.2; Biolegend) in the presence or absence of hPD-L1-Fc (20 μg/mL or 60 μg/mL), L3C7c-Fc (20 μg/mL or 60 μg/mL) or Pembrolizumab (20 μg/mL or 60 μg/mL) respectively as previously described [12].

### 2.5. Preparation of dendritic cell (DC) vaccine

Bone marrow mononuclear cells were isolated from BALB/c mice and cultured at a density of $2 \times 10^6$ cells/mL in RPMI-1640 medium supplemented with granulocyte-monocyte colony-stimulating factor (50 ng/mL; PeproTech), interleukin 4 (25 ng/mL; PeproTech) and 10% FBS at 37 °C in 5% $CO_2$. The culture medium was renewed at day 3 and

day 5. At day 5, immature DCs were pulsed with CT26 tumor lysate for 16 h, followed by the addition of tumor necrosis factor α (10 ng/mL; PeproTech) for 48 h to induce DC maturation.

### 2.6. Treatment of CT26 cell-bearing BALB/c mice

BALB/c mice were housed under specific pathogen free conditions in a 12 h light/dark cycle, and received general rodent diet and water. All experiments were carried out in accordance with a protocol approved by IACUC (No. 2013001) and Animal Welfare Assurance (No. A5748-01). On day 0, mice were subcutaneously implanted with CT26 cells ($5 \times 10^5$/mouse). On day 7, tumor-burdened mice ($n = 20$) were randomized into four groups using a Random Group Generator, each of which contained five mice. Those groups were vehicle PBS, DC vaccine, DC vaccine + L3C7c-Fc and DC vaccine + L3C7v-Fc. For all of the groups except the vehicle group, the therapeutic DC ($5 \times 10^6$/mouse) were injected subcutaneously once, and L3C7c-Fc (10 mg/kg) and L3C7v-Fc (10 mg/kg) were injected intraperitoneally every day for 11 days. Tumors were measured with callipers in two perpendicular dimensions. Tumor volumes were calculated with the following formula: volume $mm^3$ = (length × $width^2$)/2 [17]. After the final administration, mice were maintained for 2 days, then anesthetized and sacrificed.

### 2.7. Treatment of Mel624 cell-bearing NOD-SCID-B2m$^{null}$ mice

The NOD-SCID-B2m$^{null}$ mice were maintained under sterile environment-controlled conditions in a 12 h light/dark cycle and received sterilized rodent diet and water. Daily observation was performed and clinical signs were recorded. All experimental procedures were approved as described above. The mice were injected subcutaneously with Mel624 cells ($1 \times 10^6$/mouse) at day 0. At day 9, mice ($n = 25$) were randomly grouped as above and injected intravenously with human PBMCs ($2 \times 10^7$/mouse, HLA-A*0201$^+$). The groups were vehicle PBS, HATac-NYE, HATac-NYE + Pembrolizumab, HATac-NYE + L3C7c-Fc and HATac-NYE + hPD-L1-Fc. One hour after PBMCs being injected, HATac-NYE (0.07 mg/kg), Pembrolizumab (10 mg/kg), L3C7c-Fc (10 mg/kg) and hPD-L1-Fc (10 mg/kg) were administered intravenously in 100 μL PBS, and the vehicle group was administered 100 μL PBS. This was repeated every other day for 10 times. After the final administration, the mice were maintained for 6 days, then anesthetized and sacrificed. The measurement and calculation of tumors were as described above.

### 2.8. Statistical analysis

The statistical analysis and graphical presentations were computed with GraphPad Prism V5.0 software (GraphPad Software Inc.). The data were expressed as the mean ± SEM. Unpaired student's *t*-test was used to determine the statistical significance between groups, with $P < 0.05$ being considered as significant (two-tailed). The size of the samples and number of repetitions were given in the corresponding figure legends.

## 3. Results

### 3.1. Construction of high-affinity human PD-L1 variant L3C7c

The high-affinity variant called L3C7-hPD-L1 [12] was combined with three mutations, F19W, I65F and Q66S, taken from other high-affinity variants to generate a new molecule named L3C7c (Fig. 1A). Surface plasmon resonance (SPR) assay showed that L3C7c had ~167-fold greater affinity for binding to hPD-1 than wild-type hPD-L1 (Fig. 1B). L3C7c-Fc demonstrated stronger hPD-1 specific binding than hPD-L1-Fc in an ELISA assay ($P < 0.001$). However, hPD-L1-Fc and L3C7c-Fc were both coated at similar densities, as an HRP-conjugated anti-hIgG Fc antibody detected similar signals from both molecules (Fig. 1C). The competitive binding analysis showed that L3C7c-Fc significantly decreased the anti-hPD-1 antibody binding to hPD-1, which was expressed on the surface of ~34.4% of the T cells, in a dose-dependent manner. The binding curves indicated that L3C7c-Fc had greater potency than wild-type hPD-L1-Fc (Fig. 1D). These results confirmed that the strength of L3C7c-Fc binding to hPD-1 was stronger than that of hPD-L1-Fc. In addition, it has been shown that hPD-L1 can bind murine PD-1 (mPD-1) with similar affinities as the murine counterpart *in vitro* [18]. We observed that L3C7c-Fc (0.8 μM) competed with anti-mPD-1 antibody binding to mPD-1 of murine lymph node cells, significantly reducing the antibody staining signals (Fig. 1E and F). Although we performed the selections using hPD-1 as the receptor, the resultant hPD-L1 variant L3C7c-Fc could bind to mPD-1 specifically.

### 3.2. L3C7c-Fc promoted stimulated PBMC to proliferate and secrete IFN-γ

To reveal the effects of L3C7c-Fc on human PBMC proliferation and IFN-γ secretion, we detected the CFDA-SE pre-stained PBMCs after anti-CD3/CD28 stimulation with or without the presence of L3C7c-Fc, hPD-L1-Fc, or Pembrolizumab respectively. Wild-type hPD-L1-Fc inhibited the proliferation of the stimulated PBMCs in a dose-dependent manner. However, Pembrolizumab and high-affinity variant L3C7c-Fc promoted the proliferation of PBMCs at similar levels (Fig. 2A and B). On the other hand, L3C7c-Fc and Pembrolizumab increased IFN-γ expressing cell populations by ~20% and ~12.5% respectively, but the wild-type hPD-L1-Fc did not (Fig. 2C and D). The new functional feature of L3C7c-Fc, promoting PBMC IFN-γ secretion, was slightly superior to those of Pembrolizumab. Our results demonstrated that, compared with the wild type hPD-L1-Fc, L3C7c-Fc had the completely opposite effects on the activated PBMCs.

### 3.3. L3C7c-Fc enhanced HATac-NYE redirected T cells to express active and killing markers

As HATac-NYE redirected T cells expressed high levels of PD-1 while killing cancer cells (Supplemental Fig. 2), and NCI-H1299 and Mel624 cells both had stable and high expressions of membrane hPD-L1 (Supplemental Fig. 3), it is sensible to investigate the effects of L3C7c-Fc on the bi-functional molecule, especially on the T cell killing and activation markers. To compare wild-type hPD-L1 to high-affinity variant L3C7c, the relevant marker expression status was investigated with the aim of uncovering the mechanisms of L3C7c-Fc affecting HATac-NYE redirected T cells. In the presence of L3C7c-Fc, the expression of IL-2, CD25, IFN-γ, and cell membrane CD107a were increased by about 19.0%, 20.0%, 19.3%, and 49.6% respectively compared to HATac-NYE alone (Fig. 3A, B, C, D and E). These results indicated the tendency to enhance T cell proliferation [19], high-affinity IL-2R assembly [20], T cell cytotoxicity [21], and degranulation [22]. L3C7c-Fc obviously promoted all four markers more efficiently than hPD-L1-Fc ($P < 0.05$, $P < 0.01$, $P < 0.05$, $P < 0.001$; Fig. 3E). Our results revealed that L3C7c-Fc not only promoted T cells activation and proliferation, but also increased the granule-dependent (perforin/granzyme) and independent (e.g. IFN-γ) activities of CTL. These elevated marker expressions would indicate the effects of L3C7c-Fc promoting HATac-NYE redirected T cells to kill tumor cells.

### 3.4. L3C7c-Fc promoted HATac-NYE redirected tumor cell killing

It is well known that the ligation of PD-L1 to PD-1 induces T-cell exhaustion, and that antibody blockade of the PD-1 axis can reverse this effect and enhance anti-tumor immunity [6]. Therefore, we evaluated the effects of L3C7c-Fc on PD-1 axis blockade as tumor cells being killed by HATac-NYE redirected cytotoxicity. The LDH release results revealed that L3C7c-Fc significantly helped HATac-NYE to induce PBMCs' lysing of NCI-H1299 and Mel624 cells in a dose-dependent manner ($P < 0.05$, $P < 0.01$; Fig. 4A). The L3C7c-Fc effects were slightly

**A**

| Residue# | 19 | 54 | 56 | 58 | 65 | 66 | 113 | 115 | 117 | 119 |
|---|---|---|---|---|---|---|---|---|---|---|
| hPD-L1 | F T... D... | I | V | Y | W | E... | I | Q... | R | C | M | I | S | Y | G | G | A | D | Y | K | R |
| L3C7c | **W** T... D... | **E** | V | **H** | W | **F**... | **F** | **S**... | **T** | C | **L** | I | **G** | Y | **K** | G | A | D | Y | K | R |

**B**

| Clone no. | $k_{on}$ (1/Ms) | $k_{off}$ (1/s) | $K_D$ (M) | $T_{1/2}$ |
|---|---|---|---|---|
| hPD-L1 | 4.361E+04 | 7.702E-01 | 1.766E-05 | 0.9s |
| L3C7c | 1.470E+05 | 1.555E-02 | 1.058E-07 | 44.6s |

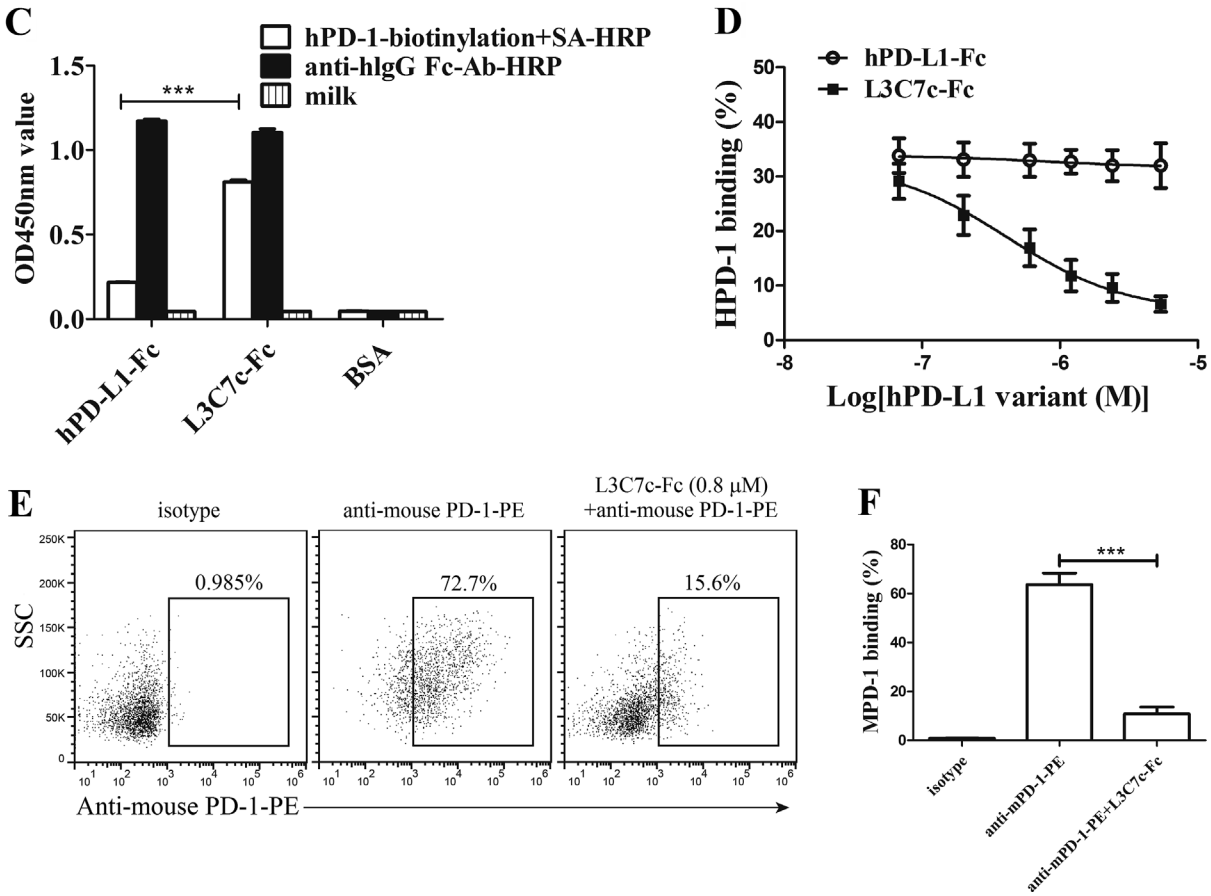


**Fig. 1.** Characteristics of L3C7c. (A) The amino acid sequences of hPD-L1 and its variant L3C7c. The mutated residues were shown in bold and the position at the original sequence was numbered. (B) The strength of the interaction between hPD-L1 or its variant L3C7c and hPD-1 as analyzed by Biacore SPR. $k_{on}$: association kinetics; $k_{off}$: dissociation kinetics; $K_D$ was a ratio of $k_{off}/k_{on}$; $T_{1/2}$: retention half-life. (C) ELISA analysis of the structure of hPD-L1-Fc and L3C7c-Fc. Pre-coated hPD-L1-Fc and L3C7c-Fc were incubated with HRP-conjugated anti-hIgG Fc antibody and hPD-1 followed with SA-HRP respectively. (D) The statistical analysis for the competition hPD-1 binding assays of hPD-L1-Fc or L3C7c-Fc with anti-human PD-1-PE. The fluorescence signal of anti-human PD-1-PE was tested by FACS for human PBMCs. The representative (E) and statistical (F) competition mPD-1 binding assays of L3C7c-Fc with anti-mouse PD-1-PE. The fluorescence signal of anti-mouse PD-1-PE was tested by FACS for murine lymph node cells. Error bars indicated SEM ($n = 3$). Unpaired student's *t*-test, $^{***}P < 0.001$; comparison was shown by brackets. Each study was repeated twice.

better than those of Pembrolizumab (Fig. 4A). Furthermore, the NCI-H1299 and Mel624 cell lysis was monitored in real-time for 72 h with an IncuCyte® zoom live cell analysis system. The intracellular insertion of YOYO®-3 iodide was monitored during the increase of the cell membrane permeability of apoptosis cells. After 72 h, the L3C7c-Fc at 10 μg/mL concentration increased the HATac-NYE redirected NCI-H1299 and Mel624 cell killing by 21.4% ($P = 0.1334$) and 66.9% ($P < 0.05$) respectively, relative to the sample without the PD-1 axis blockade (Fig. 4B). The L3C7c-Fc and Pembrolizumab demonstrated similar effects in the IncuCyte® assay (Fig. 4B). In contrast, neither L3C7c-Fc nor Pembrolizumab alone promoted the killing of cancer cells by PBMC (Fig. 4A and B). As an important part of the CTL killing mechanisms, active caspase-3 is the chief executor of cell apoptosis [23]. In the presence of L3C7c-Fc (10 μg/mL), HATac-NYE-induced NCI-H1299 intracellular active caspase-3 levels were significantly enhanced by 53.4% ($P < 0.05$) over the sample without the reagent (Fig. 4C and D). We also found that the isotype IgG4 and hPD-L1-Fc did not significantly affect the death of the tumor cells, as indicated by the LDH

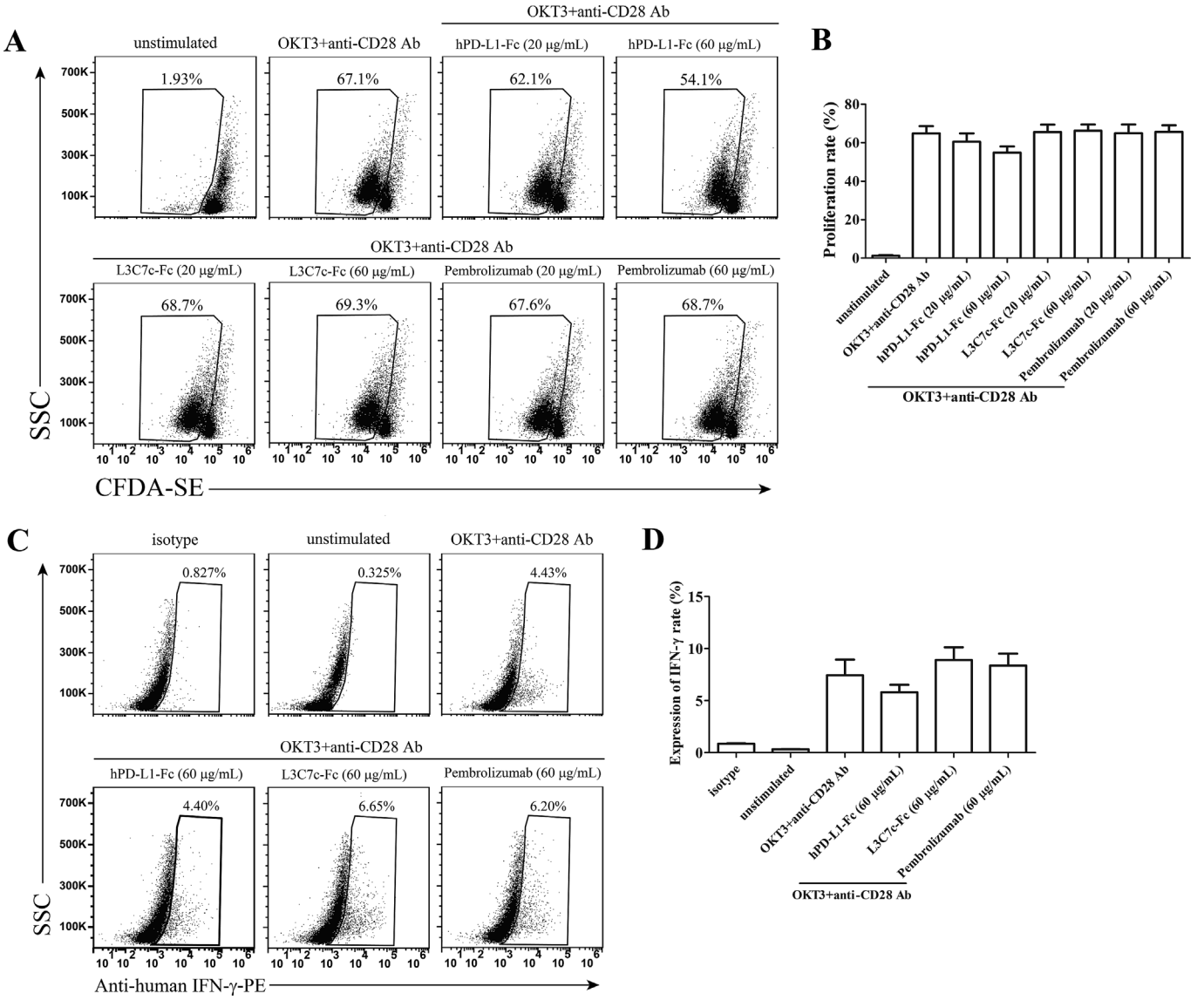


**Fig. 2.** Effects of L3C7c-Fc on PBMCs stimulated by combination of anti-CD3 and anti-CD28 antibodies. (A and C) The representative FACS data of proliferation (A) over 6 days and IFN-γ secretion (C) over 2 days of PBMCs stimulated by anti-CD3 (OKT3) and anti-CD28 antibodies in the presence of hPD-L1-Fc, L3C7c-Fc or Pembrolizumab respectively. (B and D) The statistical data of proliferation (B) and IFN-γ secretion (D) from (A) and (C) respectively. Error bars indicated SEM ($n$ = 3). Each study was repeated twice.

release (Fig. 4A), the ingestion of YOYO®-3 iodide (Fig. 4B), and the intracellular active caspase-3 levels (Fig. 4C and D). These results demonstrated that the high-affinity hPD-L1 variant L3C7c-Fc, just like the anti-PD-1 antibodies, can block PD-1 from binding PD-L1 and promote HATac-NYE redirected tumor cell killing.

### 3.5. Therapeutic efficacy of L3C7c-Fc in the humanized tumor model

Given that L3C7c-Fc effectively promoted HATac-NYE redirected T cells to kill tumor cells by antagonizing the PD-1 axis *in vitro*, we also investigated the anti-tumor effect of L3C7c-Fc *in vivo*. On the day that subcutaneously engrafted Mel624 tumors reached an average size of ~40 $mm^3$, NOD-SCID-B2$m^{null}$ humanized models were established by injecting human PBMCs intravenously once to generate an immune system response. The randomized treatment cohorts were given intravenous injections of PBS, HATac-NYE, HATac-NYE combined with Pembrolizumab, L3C7c-Fc, and hPD-L1-Fc respectively. The treatment was carried out every other day for 11 times (Fig. 5A). Supplemental Fig. 4A showed the Mel624 tumor mass from an individual NOD-SCID-B2$m^{null}$ mouse during the treatment. As expected, the Mel624 tumors in the PBS-treated mice grew rapidly (Fig. 5B and C). At the current settings, a dose of 0.07 mg/kg HATac-NYE alone only mildly inhibited Mel624 tumor growth. When the HATac-NYE treatment was stopped, the Mel624 tumor grew very fast and reached an average size equal to that of PBS group during the final six days of observation (Fig. 5B and C). However, with the assistance of L3C7c-Fc, the same doses of HATac-NYE at least doubled the inhibition of the growth of Mel624 tumors ($P$ = 0.092) (Fig. 5B and C). Comparing the effects of L3C7c-Fc and Pembrolizumab, we found that both reagents had identical ability to inhibit Mel624 tumor growth during the treatment. However, on the sixth day after stopping treatment, a significant difference was found between the L3C7c-Fc and Pembrolizumab treatment cohorts. At the end of the experiment, the antibody-treated Mel624 tumor re-grew rapidly and reached an average size only 21.5% smaller than that of the cohort without the PD-1 blockade ($P$ = 0.453). However, 6 days after the treatment was completed, the L3C7c-Fc-treated tumors showed no further growth and were about 55% smaller than the Pembrolizumab-treated groups ($P$ < 0.01) (Fig. 5B and C). The hPD-L1-Fc made no

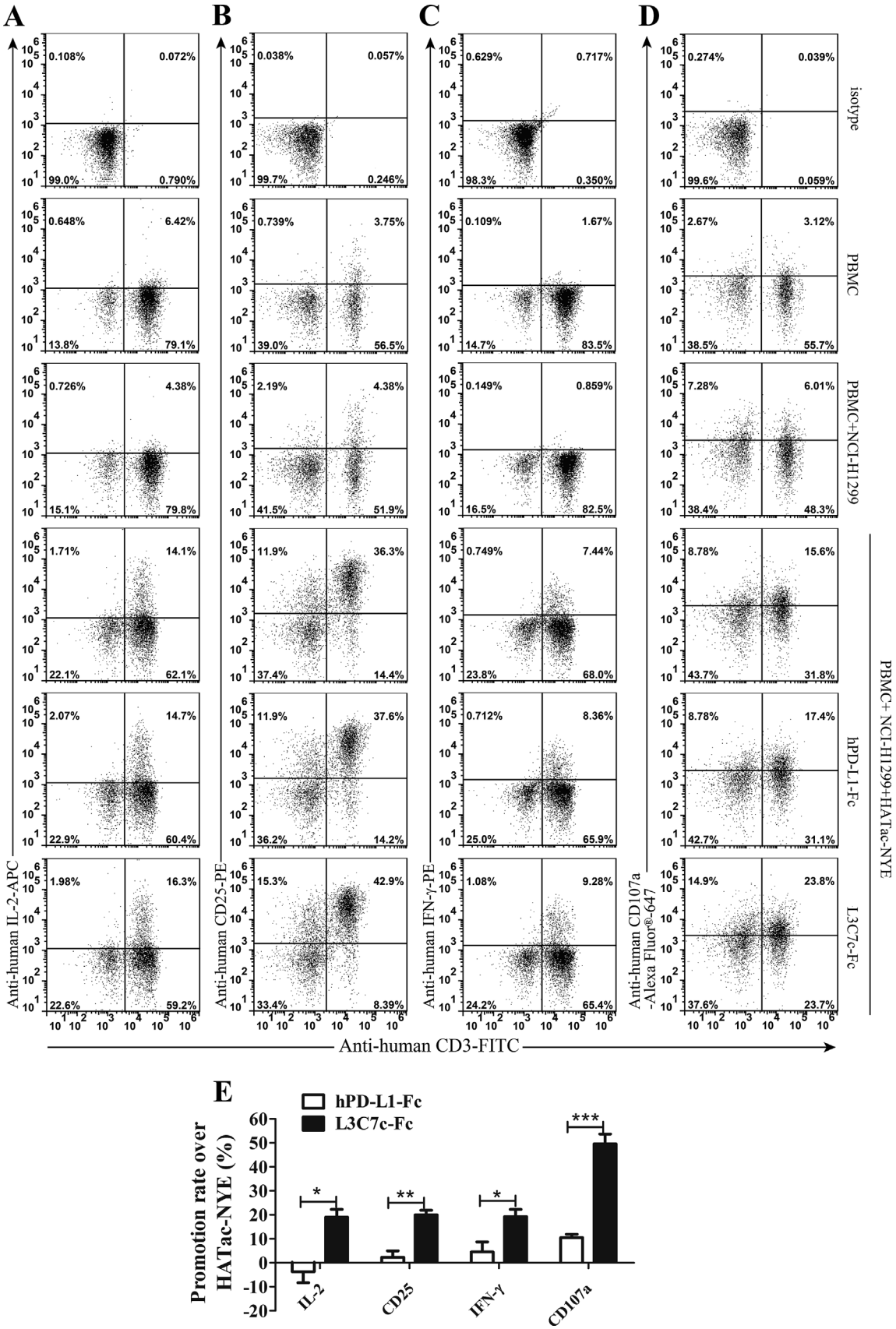


**Fig. 3.** Effects of L3C7c-Fc on the expression levels of active and killing markers of T cells stimulated by HATac-NYE. (A–D) The representative FACS data of the secretion of IL-2 (A) and IFN-γ (C), and the expression of CD25 (B) and CD107a (D) on the membrane surface of T cells. PBMCs were co-cultured with NCI-H1299 cells in the presence of HATac-NYE (1 nM) combined with hPD-L1-Fc or L3C7c-Fc for 24 h. (E) The statistical analysis on the promotion rates from (A–D). The analysis was to compare hPD-L1-Fc and L3C7c-Fc for increasing the expression of IL-2, CD25, IFN-γ and CD107a over the condition with just HATac-NYE to activate T cells. Error bars indicated SEM ($n = 3$). Unpaired student's *t*-test, $^{*}P < 0.05$; $^{**}P < 0.01$; $^{***}P < 0.001$; comparison was shown by brackets. Each study was repeated twice.

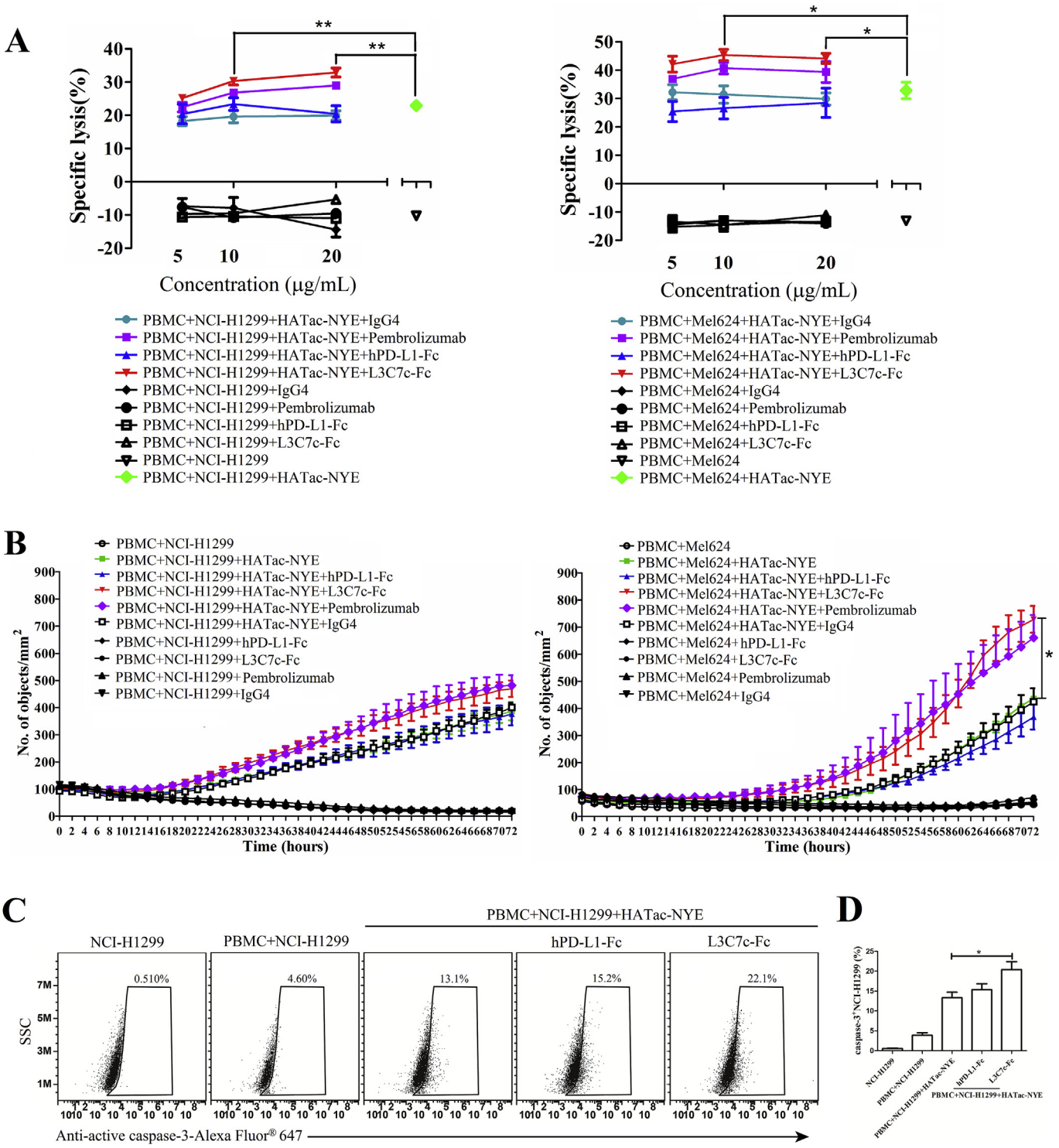


**Fig. 4.** Effects of L3C7c-Fc on HATac-NYE redirected T cells killing tumor cells. (A) The release of LDH from the co-culture system of NCI-H1299 cells or Mel624 cells and PBMCs in the presence or absence of HATac-NYE (1 nM) combined with different concentrations (5 μg/mL, 10 μg/mL and 20 μg/mL) of hPD-L1-Fc, L3C7c-Fc, Pembrolizumab or IgG4 for 24 h. (B) The intracellular fluorescence signals of YOYO®-3 iodide from NCI-H1299 cells or Mel624 cells co-cultured with PBMCs, which were in the presence or absence of HATac-NYE (1 nM) combined with 10 μg/mL of hPD-L1-Fc, L3C7c-Fc, Pembrolizumab or isotype control antibody IgG4 for 72 h. (C) The representative FACS data of the intracellular level of active caspase-3 from NCI-H1299 cells co-cultured with PBMCs, which were in the presence of HATac-NYE (1 nM) combined with 10 μg/mL of hPD-L1-Fc or L3C7c-Fc for 8 h. (D) The statistical analysis was presented for the intracellular levels of active caspase-3. Error bars indicate SEM ($n = 3$). Unpaired student's $t$-test, $^*P < 0.05$; $^{**}P < 0.01$; comparison was shown by brackets. Each study was repeated twice.

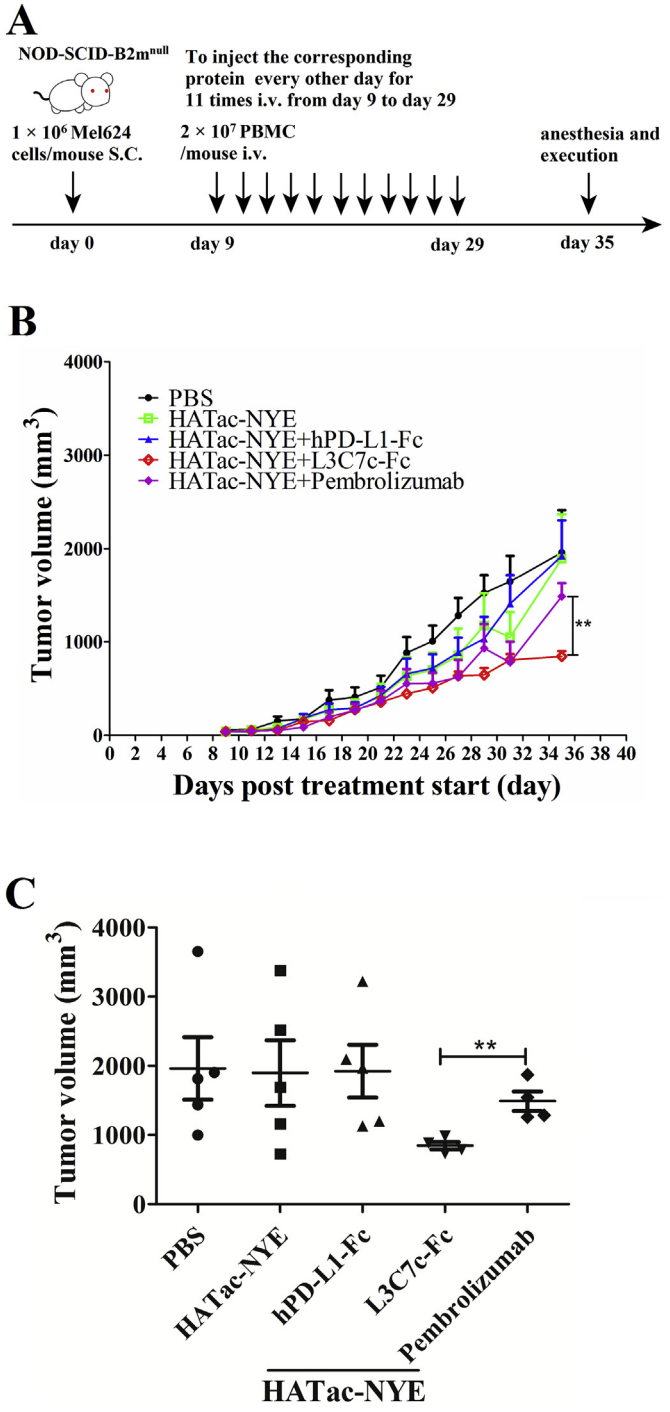


**Fig. 5.** Effects of L3C7c-Fc on assisting HATac-NYE to inhibit Mel624 tumor growth in NOD-SCID-B2m$^{null}$ mice. (A) The schematic illustration of the experimental design. Treatments were initiated for all cohorts ($n$ = 5; number of mice = 25) on day 9. The cohorts were vehicle (PBS), HATac-NYE (0.07 mg/kg), HATac-NYE (0.07 mg/kg) combined with Pembrolizumab (10 mg/kg), hPD-L1-Fc (10 mg/kg) or L3C7c-Fc (10 mg/kg) respectively. (B) Summary data for the average value of Mel624 tumor growth over the 35-day period of treatment. (C) Summary data for the average value of Mel624 tumor growth of treatment on day 35. Error bars represent SEM ($n$ = 5), unpaired student's $t$-test, $^{**}P < 0.01$; comparison was shown by brackets.

apparent difference to the HATac-NYE treatment (Fig. 5B and C). These *in vivo* studies demonstrated that L3C7c-Fc promoted the immune suppression of Mel624 tumors more effective than Pembrolizumab.

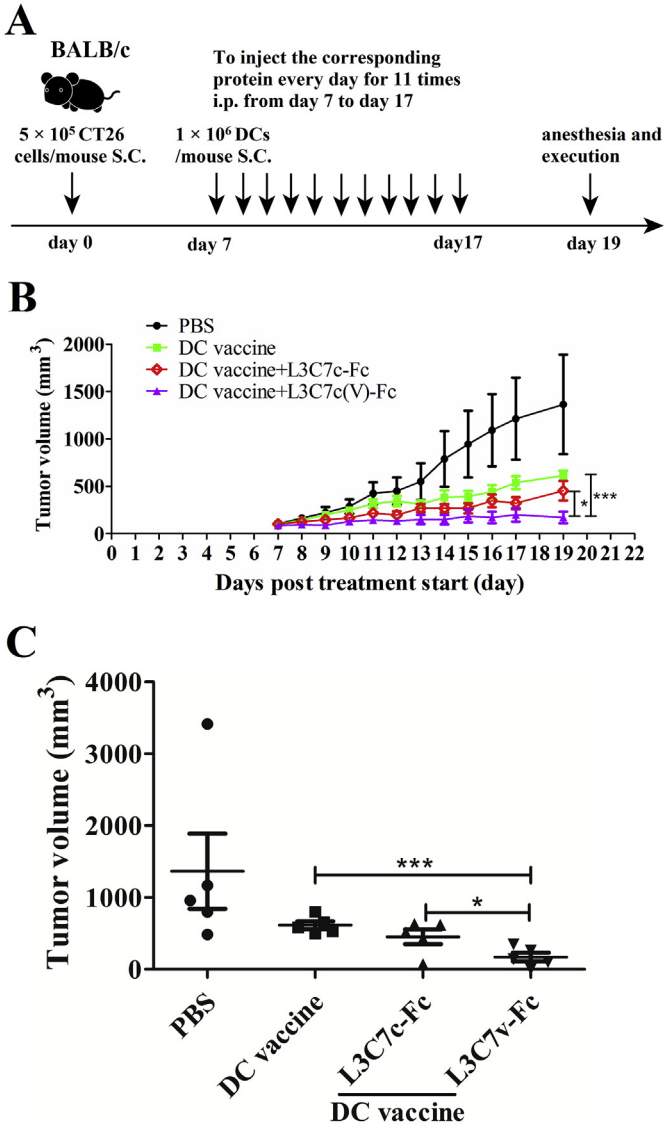


**Fig. 6.** Effects of hPD-L1 varaints on assisting DC vaccine to inhibit CT26 tumor growth in syngeneic BALB/c models. (A) The schematic illustration of the experimental design. Treatments were initiated for all cohorts ($n$ = 5; number of mice = 20) on day 7. The cohorts were vehicle (PBS), DC vaccine (once), DC vaccine (once) combined with L3C7c-Fc (10 mg/kg) or L3C7v-Fc (10 mg/kg) respectively. (B) Summary data for the average value of CT26 tumor growth over the 19-day period of treatment. (C) Summary data for the average value of CT26 tumor growth of treatment on day 19. Error bars represent SEM ($n$ = 5), unpaired student's $t$-test, $^{*}P < 0.05$; $^{***}P < 0.001$; comparison was shown by brackets. This study was repeated once.

### 3.6. Therapeutic efficacy of L3C7v-Fc in immunocompetent mouse

The relation between the size of the fusion protein and its *in vivo* efficacy for treating cancer is unclear, as in solid tumors the molecule size determines the efficacy of the therapeutic reagents [10]. To address this issue, we investigated the relation between molecular size and the synergic function under the vaccine treatment that can significantly control the growth of solid tumors [8]. The size of the L3C7c-Fc fusion protein was reduced by truncating the hPD-L1 constant domain of L3C7c. The new version of L3C7c-Fc, named L3C7v-Fc, had a molecular weight of 75 KDa, which is three-quarters that of L3C7c-Fc (100 KDa) (Supplemental Fig. 5). Analysis by competition assays showed no change in the hPD-1 binding affinity of L3C7v-Fc (Supplemental Fig. 6). In addition, compared to L3C7c-Fc, L3C7v-Fc had the same capacity for

promoting HATac-NYE redirected PBMCs to lyse NCI-H1299 and Mel624 cancer cells *in vitro* (Supplemental Fig. 7). We engrafted immunocompetent BALB/c mice with syngeneic CT26 tumors that have previously been shown to be responsive to PD-1 axis blockage [10] to evaluate the *in vivo* anti-tumor roles of the high-affinity PD-L1 variants. The treatment was initiated on day 7 post-engraftment after the tumors reached an average mass of ~100 $mm^3$. The randomized cohorts included the administration of PBS, and the DC vaccine or DC vaccine combined with L3C7c-Fc or L3C7v-Fc. The treatments with the reagents were carried out every day for 11 days by intraperitoneal injection (Fig. 6A). Supplemental Fig. 4B showed the growth of the engrafted CT26 tumors in an individual BALB/c mouse over the whole treatment period. The CT26 tumor growth was inhibited by the DC vaccine, producing an average tumor volume of 614 ± 107.6 $mm^3$, and the inhibition rate was ~55% of that of the PBS cohort, reaching a 1364 ± 1048.7 $mm^3$ average volume ($P = 0.226$) (Fig. 6B and C, Supplemental Fig. 4C). L3C7c-Fc, which interacted with mPD-1 (Fig. 1E), helped the DC vaccine, resulting in an average tumor volume of 453 ± 205.2 $mm^3$, which represented a further 26% inhibition rate over the DC vaccine alone ($P = 0.2$) (Fig. 6B and C, Supplemental Fig. 4C). The L3C7v-Fc-DC vaccine cohort suppressed the tumor to an average mass of 172 ± 120.7 $mm^3$, delivering a significant inhibition rate of 72% over the single use of DC vaccine cohort ($P < 0.001$) and ~62% over the combined use of L3C7c-Fc-DC vaccine ($P < 0.05$) (Fig. 6B and C, Supplemental Fig. 4C). These *in vivo* studies demonstrated that L3C7v-Fc more effectively helps the DC vaccine to inhibit CT26 tumor growth than L3C7c-Fc.

## 4. Discussion

The anti-tumor immune responses mediated by T lymphocyte are essential for eliminating primary tumors and controlling metastases [24]. However, the immune checkpoint-related regulative mechanisms of T cells can be hijacked by tumor cells, allowing them to escape immune surveillance [1]. In a typical example, tumor cells up-regulate PD-L1 to interact with PD-1 of infiltrated T cells that normally inhibit cytotoxicity [6]. This inhibitory function is mediated by SHP-2 (Src homology 2 based tyrosine phosphatases) and SHP-1. These two molecules are recruited to the ITSM (immunoreceptor tyrosine-based switch motif) in the PD-1 cytoplasmic tail to dephosphorylate T-cell receptor proximal signaling molecules, including Lck (lymphocyte-specific protein tyrosine kinase), ZAP-70 (ζ-associated protein of 70 kDa), PLC-γ1 (phospholipase C γ1) and PI3K (phosphatidylinositide 3-kinases) [25]. A pre-clinical study showed that blockading the PD-1 axis signaling by anti-PD-L1 antibodies enhanced T cells to secrete IFN-γ and restored cell proliferation [8]. In clinical trials, immunotherapy with anti-PD1 antibody produced cumulative patient response rates of 18% in NSCLC, 28% in melanoma, and 27% in renal cell carcinoma [26]. As the strong checkpoint inhibitory effect is associated with low affinity ligation of wild-type membrane-bound or soluble PD-L1 ectodomain to PD-1 on T cells [2,27,28], wild-type soluble PD-L1 has not been considered as a therapeutic candidate for blockading the PD-1 axis.

We have previously confirmed the suppressive effects of wild-type soluble PD-L1; however, the suppression was attenuated by alternating PD-L1 residues at the PD-1-contacting interface, which resulted in enhanced receptor binding affinity [12]. To give soluble hPD-L1 the ability to blockade the PD-1 axis, we generated a variant L3C7c with ~167 fold greater affinity than the wild-type hPD-L1 molecule (Fig. 1A and B). The potent PD-1 axis blockade molecule was constructed as an L3C7c-Fc fusion protein (Fig. 1C). As expected, the L3C7c-Fc did not have any inhibitory effect even at high concentrations. Unlike hPD-L1-Fc, which suppressed T cells, L3C7c-Fc slightly increased proliferation (Fig. 2A) and significantly enhanced the expression of IFN-γ (Fig. 2C) when the T cells were activated by stimulating the first and second signals. According to our previously reported results, it might be resulted from that insufficient signals to ITSM were generated by recruiting SHP-2 and SHP-1 through the high-affinity interaction of L3C7c-Fc and hPD-1 on the T cells [12]. In addition, the ligation of PD-1 with L3C7c-Fc prevented the PD-L1 on the target cell from binding to the PD-1 on the T cells. This should promote HATac-NYE redirected T cells to activate and express the killing factors (IFN-γ and CD107a), which could enhance HATac-NYE's ability to redirect T cells to kill tumor cells *in vitro* and *in vivo*.

Diverse T-cell effector functions are regulated by differential strengths of PD-1 signaling, which is determined by the amount of PD-1 expressed on the surface of T cells [29]. This suggests that each PD-L1-bound PD-1 molecule delivers consistent and constant inhibitory signal, which may explain why L3C7c-Fc and anti-PD-1 antibody (Pembrolizumab) restoring T-cell anti-tumor activity *in vitro* reached the platform (Fig. 4A). Pembrolizumab blocks the interaction of hPD-1 and hPD-L1 by competing with the interaction at the C′ strands of hPD-1 [30], resulting in the failure of the PD-1 signal. Based on our results, we propose that, unlike soluble wild-type hPD-L1, PD-1 axis signals cannot be generated while the high-affinity PD-L1 variant L3C7c-Fc binds hPD-1 on T cells. These mechanisms allowed L3C7c-Fc and Pembrolizumab to consistently reverse the exhausted T-cell functions *in vitro* and *in vivo*. In contrast to the L3C7c-Fc-HATac-NYE combination, it was intriguing that the therapeutic effect of Pembrolizumab-HATac-NYE declined rapidly once the treatment was stopped in NOD-SCID-B2m$^{null}$ mice. The resultant Pembrolizumab-treated tumor was significantly larger than that of L3C7c-Fc-treated samples on the day of anesthesia and execution. The mechanism that created this discrepancy is outside the scope the current investigation, but should be examined in future studies. However, we noted that the L3C7c-Fc function was clear but not significantly better than the antibody in terms of promoting T cell proliferation, IFN-γ expression, and cytotoxicity of Mel624 cells *in vitro*. For the solid tumor, we believe that the tumor clearance requires a strong force to swiftly overcome the tumor growth and to reduce the opportunity for the tumor to escape from the immune system's control. The small advantage of L3C7c in proliferation, cytokine expression, and cytotoxicity may play a big role in suppressing the tumor growth in the current condition.

It is well known that the tissue permeability in a tumor microenvironment is a very important factor in the success rates of the clinic applications of reagents [10,31]. Smaller macromolecular reagents achieve better tissue penetration [31]. A previous study found that the tumor penetration of one PD-1 variant (HAC-PD-1) was more effective than that of the anti-PD-L1 antibody, which had nearly twice the molecular weight. Due to its smaller size, HAC-PD-1 had a superior anti-tumor effect *in vivo* than the antibody [10]. Our study showed that compared to the L3C7c-Fc fusion protein, L3C7v-Fc had superior *in vivo* efficacy with only a 25% smaller size of ~75 kDa. Apart from the size difference, we did not observe any functional difference between L3C7c-Fc and L3C7v-Fc. Therefore, we believe that better penetration may be the factor that makes the anti-tumor effect of L3C7v-Fc in synergizing DC vaccine significantly stronger than that of L3C7c-Fc (Fig. 6B and C, Supplemental Fig. 4C).

In conclusion, this is the first study to show that the high-affinity soluble hPD-L1 variant L3C7c can blockade the suppressive effect of the hPD-1 axis. The penetration of the reagent may play an important role in achieving optimal tumor therapeutic efficacy. Future studies are needed to evaluate the potential of L3C7c-Fc and L3C7v-Fc as new kind of cancer immunotherapy reagents.

### Conflicts of interest statement

The authors declare no potential conflicts of interest.

### Conflicts of interest

None.

## Author contributions

Y.L. and Z.D.L. planned the project, designed the experiments, and analyzed and interpreted the data. Z.D.L., Y.Y. L., Y.T., H.L.Z., W.X.C., A.A.C., L.C., Y.F.B., and B.X. performed the experiments and collected data. H.P.K. contributed expertise. Z.D.L. and Y.L. wrote and reviewed the paper. Y.L. approved the final version submitted for publication.

## Funding

This work was supported by the Science and Technology Program of Guangzhou [grant numbers 201504010016]; National Key R&D Program [grant numbers 2016YFC1303404]; and Science and Technology Program of Guangzhou [grant numbers 201704020220].

## Acknowledgments

We thank Xianhui Wu for technical assistance with the expression and purification of hPD-L1-Fc, and Hui Fan for providing important reagents.

## Appendix A. Supplementary data

Supplementary data to this article can be found online at https://doi.org/10.1016/j.canlet.2019.01.016.

## References

[1] D.M. Pardoll, The blockade of immune checkpoints in cancer immunotherapy, Nat. Rev. Canc. 12 (2012) 252–264.
[2] G.J. Freeman, A.J. Long, Y. Iwai, K. Bourque, T. Chernova, H. Nishimura, L.J. Fitz, N. Malenkovich, T. Okazaki, M.C. Byrne, H.F. Horton, L. Fouser, L. Carter, V. Ling, M.R. Bowman, B.M. Carreno, M. Collins, C.R. Wood, T. Honjo, Engagement of the PD-1 immunoinhibitory receptor by a novel B7 family member leads to negative regulation of lymphocyte activation, J. Exp. Med. 192 (2000) 1027–1034.
[3] J.R. Kim, Y.J. Moon, K.S. Kwon, J.S. Bae, S. Wagle, K.M. Kim, H.S. Park, H. Lee, W.S. Moon, M.J. Chung, M.J. Kang, K.Y. Jang, Tumor infiltrating PD1-positive lymphocytes and the expression of PD-L1 predict poor prognosis of soft tissue sarcomas, PLoS One 8 (2013) e82870.
[4] H. Ghebeh, S. Mohammed, A. Al-Omair, A. Qattan, C. Lehe, G. Al-Qudaihi, N. Elkum, M. Alshabanah, S. Bin Amer, A. Tulbah, D. Ajarim, T. Al-Tweigeri, S. Dermime, The B7-H1 (PD-L1) T lymphocyte-inhibitory molecule is expressed in breast cancer patients with infiltrating ductal carcinoma: correlation with important high-risk prognostic factors, Neoplasia 8 (2006) 190–198.
[5] H. Nishimura, M. Nose, H. Hiai, N. Minato, T. Honjo, Development of lupus-like autoimmune diseases by disruption of the PD-1 gene encoding an ITIM motif-carrying immunoreceptor, Immunity 11 (1999) 141–151.
[6] H. Dong, S.E. Strome, D.R. Salomao, H. Tamura, F. Hirano, D.B. Flies, P.C. Roche, J. Lu, G. Zhu, K. Tamada, V.A. Lennon, E. Celis, L. Chen, Tumor-associated B7-H1 promotes T-cell apoptosis: a potential mechanism of immune evasion, Nat. Med. 8 (2002) 793–800.
[7] F. Hirano, K. Kaneko, H. Tamura, H. Dong, S. Wang, M. Ichikawa, C. Rietz, D.B. Flies, J.S. Lau, G. Zhu, K. Tamada, L. Chen, Blockade of B7-H1 and PD-1 by monoclonal antibodies potentiates cancer therapeutic immunity, Cancer Res. 65 (2005) 1089–1096.
[8] Y. Ge, H. Xi, S. Ju, X. Zhang, Blockade of PD-1/PD-L1 immune checkpoint during DC vaccination induces potent protective immunity against breast cancer in hu-SCID mice, Cancer Lett. 336 (2013) 253–259.
[9] C. Zhang, S. Wu, X. Xue, M. Li, X. Qin, W. Li, W. Han, Y. Zhang, Anti-tumor immunotherapy by blockade of the PD-1/PD-L1 pathway with recombinant human PD-1-IgV, Cytotherapy 10 (2008) 711–719.
[10] R.L. Maute, S.R. Gordon, A.T. Mayer, M.N. McCracken, A. Natarajan, N.G. Ring, R. Kimura, J.M. Tsai, A. Manglik, A.C. Kruse, S.S. Gambhir, I.L. Weissman, A.M. Ring, Engineering high-affinity PD-1 variants for optimized immunotherapy and immuno-PET imaging, Proc. Natl. Acad. Sci. U. S. A. 112 (2015) E6506–E6514.
[11] M. Muller, R.D. Schouten, C.J. De Gooijer, P. Baas, Pembrolizumab for the treatment of non-small cell lung cancer, Expert Rev. Anticancer Ther. 17 (2017) 399–409.
[12] Z. Liang, Y. Tian, W. Cai, Z. Weng, Y. Li, H. Zhang, Y. Bao, Y. Li, High-affinity human PD-L1 variants attenuate the suppression of T cell activation, Oncotarget 8 (2017) 88360–88375.
[13] H. Zhang, J. Zhang, L. Chen, Z. Weng, Y. Tian, H. Zhao, Y. Li, L. Chen, Z. Liang, H. Zheng, W. Zhao, S. Zhong, Y. Li, Targeting naturally occurring epitope variants of hepatitis C virus with high-affinity T-cell receptors, J. Gen. Virol. 98 (2017) 374–384.
[14] J. Duraiswamy, K.M. Kaluza, G.J. Freeman, G. Coukos, Dual blockade of PD-1 and CTLA-4 combined with tumor vaccine effectively restores T-cell rejection function in tumors, Cancer Res. 73 (2013) 3591–3603.
[15] X. Yang, F. Wang, Y. Zhang, L. Wang, S. Antonenko, S. Zhang, Y.W. Zhang, M. Tabrizifard, G. Ermakov, D. Wiswell, M. Beaumont, L. Liu, D. Richardson, M. Shameem, A. Ambrogelly, Comprehensive analysis of the therapeutic IgG4 antibody Pembrolizumab: hinge modification blocks half molecule exchange in vitro and in vivo, J. Pharmacol. Sci. 104 (2015) 4002–4014.
[16] E. McCormack, K.J. Adams, N.J. Hassan, A. Kotian, N.M. Lissin, M. Sami, M. Mujic, T. Osdal, B.T. Gjertsen, D. Baker, A.S. Powlesland, M. Aleksic, A. Vuidepot, O. Morteau, D.H. Sutton, C.H. June, M. Kalos, R. Ashfield, B.K. Jakobsen, Bi-specific TCR-anti CD3 redirected T-cell targeting of NY-ESO-1- and LAGE-1-positive tumors, Cancer Immunol. Immunother. 62 (2013) 773–785.
[17] R. Winograd, K.T. Byrne, R.A. Evans, P.M. Odorizzi, A.R. Meyer, D.L. Bajor, C. Clendenin, B.Z. Stanger, E.E. Furth, E.J. Wherry, R.H. Vonderheide, Induction of T-cell immunity overcomes complete resistance to PD-1 and CTLA-4 blockade and improves survival in pancreatic carcinoma, Cancer Immunol Res 3 (2015) 399–411.
[18] D.Y. Lin, Y. Tanaka, M. Iwasaki, A.G. Gittis, H.P. Su, B. Mikami, T. Okazaki, T. Honjo, N. Minato, D.N. Garboczi, The PD-1/PD-L1 complex resembles the antigen-binding Fv domains of antibodies and T cell receptors, Proc. Natl. Acad. Sci. U. S. A. 105 (2008) 3011–3016.
[19] S.L. Gaffen, K.D. Liu, Overview of interleukin-2 function, production and clinical applications, Cytokine 28 (2004) 109–123.
[20] T.R. Malek, I. Castro, Interleukin-2 receptor signaling: at the interface between tolerance and immunity, Immunity 33 (2010) 153–165.
[21] P. Bhat, G. Leggatt, N. Waterhouse, I.H. Frazer, Interferon-gamma derived from cytotoxic lymphocytes directly enhances their motility and cytotoxicity, Cell Death Dis. 8 (2017) e2836.
[22] M.R. Betts, J.M. Brenchley, D.A. Price, S.C. De Rosa, D.C. Douek, M. Roederer, R.A. Koup, Sensitive and viable identification of antigen-specific CD8+ T cells by a flow cytometric assay for degranulation, J. Immunol. Methods 281 (2003) 65–78.
[23] J. Thiery, S. Abouzahr, G. Dorothee, A. Jalil, C. Richon, I. Vergnon, F. Mami-Chouaib, S. Chouaib, p53 potentiation of tumor cell susceptibility to CTL involves Fas and mitochondrial pathways, J. Immunol. 174 (2005) 871–878.
[24] S.R. Woo, M.E. Turnis, M.V. Goldberg, J. Bankoti, M. Selby, C.J. Nirschl, M.L. Bettini, D.M. Gravano, P. Vogel, C.L. Liu, S. Tangsombatvisit, J.F. Grosso, G. Netto, M.P. Smeltzer, A. Chaux, P.J. Utz, C.J. Workman, D.M. Pardoll, A.J. Korman, C.G. Drake, D.A. Vignali, Immune inhibitory molecules LAG-3 and PD-1 synergistically regulate T-cell function to promote tumoral immune escape, Cancer Res. 72 (2012) 917–927.
[25] V.A. Boussiotis, Molecular and biochemical aspects of the PD-1 checkpoint pathway, N. Engl. J. Med. 375 (2016) 1767–1778.
[26] S.L. Topalian, F.S. Hodi, J.R. Brahmer, S.N. Gettinger, D.C. Smith, D.F. McDermott, J.D. Powderly, R.D. Carvajal, J.A. Sosman, M.B. Atkins, P.D. Leming, D.R. Spigel, S.J. Antonia, L. Horn, C.G. Drake, D.M. Pardoll, L. Chen, W.H. Sharfman, R.A. Anders, J.M. Taube, T.L. McMiller, H. Xu, A.J. Korman, M. Jure-Kunkel, S. Agrawal, D. McDonald, G.D. Kollia, A. Gupta, J.M. Wigginton, M. Sznol, Safety, activity, and immune correlates of anti-PD-1 antibody in cancer, N. Engl. J. Med. 366 (2012) 2443–2454.
[27] X. Cheng, V. Veverka, A. Radhakrishnan, L.C. Waters, F.W. Muskett, S.H. Morgan, J. Huo, C. Yu, E.J. Evans, A.J. Leslie, M. Griffiths, C. Stubberfield, R. Griffin, A.J. Henry, A. Jansson, J.E. Ladbury, S. Ikemizu, M.D. Carr, S.J. Davis, Structure and interactions of the human programmed cell death 1 receptor, J. Biol. Chem. 288 (2013) 11771–11785.
[28] X. Frigola, B.A. Inman, C.M. Lohse, C.J. Krco, J.C. Cheville, R.H. Thompson, B. Leibovich, M.L. Blute, H. Dong, E.D. Kwon, Identification of a soluble form of B7-H1 that retains immunosuppressive activity and is associated with aggressive renal cell carcinoma, Clin. Canc. Res. 17 (2011) 1915–1923.
[29] F. Wei, S. Zhong, Z. Ma, H. Kong, A. Medvec, R. Ahmed, G.J. Freeman, M. Krogsgaard, J.L. Riley, Strength of PD-1 signaling differentially affects T-cell effector functions, Proc. Natl. Acad. Sci. U. S. A. 110 (2013) E2480–E2489.
[30] S. Tan, D. Chen, K. Liu, M. He, H. Song, Y. Shi, J. Liu, C.W. Zhang, J. Qi, J. Yan, S. Gao, G.F. Gao, Crystal clear: visualizing the intervention mechanism of the PD-1/PD-L1 interaction by two cancer therapeutic monoclonal antibodies, Protein Cell 7 (2016) 866–877.
[31] T. Ying, T.W. Ju, Y. Wang, P. Prabakaran, D.S. Dimitrov, Interactions of IgG1 CH2 and CH3 domains with FcRn, Front. Immunol. 5 (2014) 146.